Landscape configuration of an Amazonian island-like ecosystem drives population structure and genetic diversity of a habitat-specialist bird

Camila D. Ritter[1*], Camila C. Ribas[2], Juliana Menger[2], Sergio H. Borges[3] Christine D. Bacon[4,5], Jean P. Metzger[6], John Bates[7], Cintia Cornelius[3]

Author affiliations

[1] Department of Eukaryotic Microbiology, University of Duisburg-Essen, Universitätsstrasse 5 D-45141 Essen, Germany

[2] Coordenação de Biodiversidade e Coleções Zoológicas, Instituto Nacional de Pesquisas da Amazônia, Av. André Araújo 2936, Manaus, AM 69060-001, Brazil

[3] Universidade Federal do Amazonas, Av. Rodrigo Otávio Jordão Ramos 3000, Bloco E, Setor Sul, Manaus, AM 69077-000, Brazil

[4] Department of Biological and Environmental Sciences, University of Gothenburg, Box 463, 405 30 Göteborg, Sweden.

[5] Gothenburg Global Biodiversity Centre, Box 461, SE-405 30 Göteborg, Sweden.

[6] Departamento de Ecologia, Instituto de Biociências, Universidade de São Paulo, Rua do Matão, 321, travessa 14, São Paulo, SP 05508-900, Brazil

[7] Life Sciences Section, Negaunee Integrative Research Center, The Field Museum of Natural History, 1400 S. Lake Shore Drive, Chicago, IL 60605, USA

*Corresponding author

Camila D. Ritter, kmicaduarte@gmail.com. Phone: +55 48991434597. Postal address: University of Duisburg-Essen, Universitätsstrasse 5 - D-45141 Essen, Germany. ORCID: 0000-0002-3371-7425.

Abstract

Context: Amazonian white-sand ecosystems (*campinas*) are open vegetation patches which form a natural island-like system in a matrix of tropical rainforest. Due to their clear distinction from the surrounding matrix, the spatial characteristics of *campina* patches may affect the genetic diversity and composition of their specialized organisms such as the small and endemic passerine *Elaenia ruficeps*.

Objectives: Here, we estimate the relative contribution of the current extension, configuration and geographical context of *campina* patches to the patterns of genetic diversity and population structure of *E. ruficeps*.

Methods: We sampled individuals of *E. ruficeps* from three landscapes in Central Amazonia with contrasting *campina* spatial distribution, from landscapes with large and connected patches to landscapes with small and isolated patches. We estimate population structure, genetic diversity, and contemporary and historical migration within and among the three landscapes and used landscape metrics as predictor variables. Furthermore, we estimate genetic isolation by distance and resistance among individuals sampled within landscapes.

Results: We identified three genetically distinct populations with asymmetrical gene flow among landscapes and a decreasing migration rate with distance. Within each landscape, we found low genetic differentiation without genetic isolation by distance nor by resistance. In contrast, we found differentiation and spatial correlation between landscapes.

Conclusions: Our results uncover population dynamics of *E. ruficeps* through time. Together with previous studies, this suggests that both regional context and landscape structure shape the connectivity among populations of *campina* specialist birds, and that Amazonian landscapes, together with their associated biota, have responded to recent climatic changes.

Keywords: *Campinas*, *Elaenia ruficeps*, landscape genetics, migration, spatial isolation.

Introduction

50

51 Landscapes are mosaics of environments with distinct structure and biotic composition. Natural

52 island-like systems such as habitat patches, caves, and mountaintops provide important

53 contributions to landscape structure and diversity (Itescu 2019). Due to their well-defined borders

54 and distinction from the surrounding habitats, the spatial characteristics of island-like systems may

55 influence biological assemblages and their attributes including the genetic diversity and

56 differentiation. These island-like systems can vary in the extent of insularity they impose on the

57 taxa they harbor, affecting the extent to which organisms can disperse and colonize new patches

58 (Itescu 2019).

59

60 Amazonia has the highest biodiversity among all tropical rainforests and is a global biodiversity

61 hotspot (Hansen et al. 2013). The predominant view of Amazonia as a homogeneous humid

62 tropical forest does not match the heterogeneity of landscapes it harbors (Myster 2016; Tuomisto

63 et al. 2019). Indeed, Amazonia comprises diverse vegetation formations from humid tropical

64 forests (*terra-firme*) to non-forested formations, such as white-sand grasslands and shrubby

65 habitats (Anderson 1981; Adeney et al. 2016; Capurucho et al. 2020a).

66

67 White-sand shrub and grassland patches, hereafter *campinas*, are naturally fragmented and

68 resemble islands in a "sea" of forests, growing on nutrient-poor soils (Prance 1996; Fine et al.

69 2010; Ritter et al. 2018; Costa et al. 2020; Capurucho et al. 2020a). *Campina* patches cover

70 approximately 1.6% of the Amazon basin (Adeney et al. 2016), yet are an important Amazonian

71 island-like system, harboring a unique biota (Borges et al. 2016a; Costa et al. 2020; Capurucho et

72 al. 2020a). Landscapes with *campina* patches have different spatial configurations throughout

73 Amazonia, composed of large and connected patches in the north and small and isolated patches

74 in the south (Borges et al. 2016a).

75

76   Moreover, properties of *campina* landscapes, such as habitat amount, patch isolation and matrix

77   properties, vary across space and time. As such, it is expected that gene flow among populations

78   and hence genetic diversity of populations inhabiting *campina* patches will depend on the structure

79   of these landscapes. Thus, landscapes with more *campina* habitat cover and with connected patches

80   should harbor a higher genetic diversity than landscapes with reduced habitat and isolated patches.

81   However, the effects of landscape configuration on the organisms that thrive in naturally

82   fragmented *campinas* remain poorly understood (but see Capurucho et al. 2013; Borges et al.

83   2016a).

84

85   Several factors may restrict the movement of individuals in island-like systems, such as *campinas*.

86   In naturally heterogeneous landscapes, restrictions of movement and gene flow can be due, for

87   instance, to geographic distance (isolation by distance; Wright 1943), or to non-suitable habitat

88   (isolation by resistance; e.g. McRae 2006; DiLeo and Wagner 2016). Dispersal promotes gene

89   flow and connects geographically isolated populations, increases genetic diversity, and reduces

90   inbreeding (Ronce 2007). However, dispersal through non-suitable habitats also represents high

91   energetic costs and mortality risks (Fahrig 1998; Gruber and Henle 2008).

92

93   The geographical distance between patches, within and among landscapes, and the type and

94   configuration of environments in the matrix may affect the ability of a species to disperse (Bates

95   2002). Different matrices create variable resistance to individuals' movement (Itescu 2019). In

96   Amazonia, white water rivers, such as the Amazon River, appear to impose large resistance for

97   white-sand vegetation specialist birds (Capurucho et al. 2013; Matos et al. 2016; Ritter et al. 2020).

98   However, little is known about how composition and configuration of *campina* landscapes shape

99   movements of specialist species. Also, landscapes are dynamic over time and thus movement

100   patterns of individuals may differ within and among landscapes over time (Manicacci et al. 1992).

101   Understanding these movements through time provides information on landscape configuration

102   changes in the past, contributing to the long debate about stability of Amazonian habitats during

103   the Quaternary (Cheng et al. 2013; Wang et al. 2017; Bicudo et al. 2019; Rocha and Kaefer 2019).

104

105   Methods of molecular analyses have been successfully used to investigate patterns and to infer

106   processes related to the origin and maintenance of biodiversity (e.g. Antonelli et al. 2018; Silva et

107   al. 2019). The use of gene sequencing can reveal historical patterns through phylogeographic

108   studies (Avise 2009). On the other hand, the genotyping of microsatellite markers can reveal

109   contemporary patterns, because they are highly polymorphic due to their high mutational rate

110   (Tautz 1989), and therefore have been considered ideal for studies of contemporary population

111   structure (Frankham et al. 2002). In this context, the use of molecular markers with distinct

112   evolutionary rates may uncover how the interaction between landscape features and micro-

113   evolutionary processes shapes patterns of genetic structure and diversity in time and space

114   (Capurucho et al. 2013).

115

116   In this study we investigate the effects of landscape configuration on population genetic structure

117   and diversity in a white-sand vegetation specialist bird species restricted to Amazonian *campina*

118   patches, *Elaenia ruficeps* (Aves: Tyrannidae; Rheindt, Norman and Christidis 2008; Borges et al.

119   2016b), employing mitochondrial gene sequences and microsatellite markers.

120

121   We address the following questions:

122   (1) How do genetic diversity, population structure, and migration rates differ within and among

123   three *campina* landscapes with contrasting configuration? We expect differences between genetic

124   metrics measured through markers with faster (microsatellites) and slower (DNA sequence)

125   evolutionary rates that responded to processes at different time scales, with microsatellites more

126   congruent with current landscape structure.

127   (2) How does habitat amount and isolation of patches within and among landscapes affect

128   population genetic diversity in *E. ruficeps?* We expect that both metrics will be important but

129   habitat amount will be the strongest factor explaining genetic diversity.

130   (3) What is the relative importance of geographical distance and matrix resistance in limiting gene

131   flow in *E. ruficeps?* We expected that habitat matrix resistance will better explain genetic

132   differentiation among populations than geographic distance. We explicitly tested if *terra-firme*

133   *forest* and rivers limited movement of *E. ruficeps* individuals more than other landscape matrix

134   types, such as seasonally flooded forests.

135

136   **Materials and Methods**

137

138   *Study area*: We sampled birds in three landscapes (each *ca* 50 x 50 km) north of the Amazon River

139   (Fig. 1A): Aracá (0°28'7.76" N, 63°28'32.20" W; Fig. 1B), Viruá (1º36' N, 61º13' W; Fig. 1C),

140   and Uatumã (2°17'9.19" S, 58°51'53.92" W; Fig. 1D). The Aracá landscape lies on the eastern

141   side of the middle part of the Negro river basin on the western margin of the Branco river (i.e. in

142   the Branco-Negro interfluve) and has the highest *campina* vegetation coverage (45.33% of its area

143   in 50 x 50 km^2) distributed as large and connected patches. The Viruá landscape is located on the

144   eastern margin of the Branco River, and has intermediate *campina* vegetation coverage (28.2 % of

145   its area) distributed as both large and small interconnected patches. This is the only site with

146   anthropogenic disturbance due to an interstate road and a few secondary non-paved roads among

147   the sampling sites. The third and southernmost landscape, Uatumã, is located on the banks of the

148   Uatumã river, inside the limits of the Uatumã Sustainable Development Reserve. The Uatumã

149   landscape has less *campinas* coverage (0.8% of its area) with small and isolated *campina* patches

150   (Fig. 1 B-D). We established six sampling sites within the Aracá landscape, six sampling sites

151   within the Uatumã landscapes, and four sampling sites within the Viruá landscape, with a total of

152   16 sampling sites. These sites were distributed across landscapes in *campinas* vegetation with

153   distances ranging from 5 to 44 km among them within landscapes, as described in Capurucho et

154   al. (2013) and Borges et al. (2016a).

155

156   *Landscape metrics:* We used categorical maps with six pre-defined classes: *terra-*

157   *firme forest*, *campinas*, *campinarana* (white-sand patches with taller vegetation coverage than

158   *campinas*), flooded forest, water, and anthropogenic areas (see Capurucho et al. 2013 for details

159   on the classification method). We used ArcGIS v.9.1 (Press 2005) and Fragstas v.3.4 (McGarigal

160   et al. 2002) to calculate two landscapes metrics. The first was a habitat amount metric calculated

161   as the area of *campina* vegetation in a radius of 5 km around each sampling site. As a configuration

162   metric, we used the proximity index, an isolation measure of each patch in which sampling sites

163   were located, that was based on the sum of the area of neighboring patches within a 5 km search

164   radius, weighted by the distance to neighboring patches (Gustafson and Parker 1994). The 5 km

165   radius was selected based on dispersal kernels described for several Neotropical bird species; most

166   Amazonian birds disperse less than 5 km (Van Houtan et al. 2007). Habitat amount and proximity

167   index were not correlated (Pearson correlation = 0.3, p = 0.24).

168

169   *Sampling*: We defined sampling area as a 500 m radius circle centered at each sampling site, in

170   which 20 mist-nets (12 m long, 36 mm mesh size) were equally distributed into four mist-net lines.

171   In order to reduce the probability of sampling only one family group, at least two mist-net lines

172   were moved each day to cover other parts of the sampling sites. Sampling was conducted during

173   the dry season of 2010 and 2011, and each site was sampled as many days as needed to capture at

174   least 10 individuals per site, ranging from 2-5 days per site, but in four sites the intended number

175   of individuals was not attained (see Table S1). A blood sample (~ 50 µl) was taken from each

176   captured individual, stored in ethanol, and deposited in the Genetic Resources Collection of the

177   National Institute for Amazonian Research (INPA, Manaus, Brazil). Voucher specimens

178   (maximum of five per landscape) were also collected and deposited at INPA Bird Collection

179   (Table S1).

180

181   *DNA sequencing*: DNA was extracted from blood or tissue samples using Promega DNA

182   Purification Kit (A1125). The complete sequence of the mitochondrial NADH Dehydrogenase 2

183   (ND2) gene was amplified using the external primers L5204 and H6313 (Sorenson et al. 1999).

184   For this study, we also designed a primer for reverse gene sequencing (H1031; 5'-

185   TAGGATTGTAGGGGATAAAGGTA-3 '), because some samples did not amplify well with

186   H6313. Amplification and sequencing details are described in Capurucho et al. (2013). Contiguous

187   sequences were assembled and aligned in Geneious v. 5.6.5 (Biomatters 2012).

188

189   *Microsatellite genotyping*: All individuals of *E. ruficeps* were genotyped at 15 microsatellite loci

190   described in Ritter et al. (2014), using protocols and PCR conditions therein. PCR products were

191   run on an ABI PRISM 3730 DNA Analyzer; size scoring was performed with GeneMarker®

192   v2.2.0 (Hulce et al. 2011). We calculated the number of alleles per locus, observed and expected

193   heterozygosity (H_o and H_e), deviations from Hardy–Weinberg equilibrium (HWE), and the exact

194   tests of linkage disequilibrium between pairs of loci for the three landscapes using Genepop Web

195   v.4.2 (Raymond and Rousset 1995; Rousset 2008; Table S2).

196

197   *Genetic diversity, population structure, and migration rates*: To investigate if genetic diversity

198   varies within and among landscapes we calculated four genetic diversity metrics (two based on

199   mitochondrial and two on microsatellite data). For each locality (both landscapes and sites within

200 each landscape) we estimated the individuals nucleotide diversity (P_i) and haplotype diversity (H_D)

201 based on ND2 mitochondrial sequences using DnaSP v.5.10.01 (Librado and Rozas 2009). For the

202 microsatellite data we estimated allelic richness using the rarefaction method implemented in the

203 *Hierfstat* v.0.4.22 package (Goudet and Jombart 2015) in R v.3.2.5 (R Core Team 2015), and

204 calculated the microsatellite genetic diversity (Theta) using Arlequin v.3.11 (Excoffier et al. 2005).

205

206 To describe historical population structure within and among landscapes, we constructed

207 haplotype networks with ND2 sequences, with all individuals together and for individuals from

208 each landscape separately, using a minimum spanning network (Clement et al. 2002) with Popart

209 v.1.7 (Leigh and Bryant 2015). We used BAPS v.6.0 (Bayesian Analysis of Population Structure;

210 (Corander et al. 2013) to infer the number of clusters (*K*) based on the mitochondrial data using all

211 individuals. Likelihood values of the mixture analysis were calculated three times for each number

212 *K* of subpopulations, ranging from 1 to 20 (since the sites number was 16 and we expected no more

213 than 20 population), accepting the partition with *K* value with higher likelihood, which were run

214 until achieving convergence.

215

216 To describe current population structure within and among landscapes, we used microsatellite data.

217 We used Structure v.2.3.4 (Pritchard et al. 2000), to infer the number of genetically distinct

218 populations (*K*). We assumed an admixture model with correlated allele frequencies and the

219 LOCPRIOR model (Hubisz et al. 2009). We used two LOCPRIOR options, first, we made analyses

220 at the landscape level, where Aracá, Viruá and Uatumã were considered each a single locality.

221 Secondly, we analyzed the data using each sampling site as unique localities. To identify the best

222 estimate of *K* from 1 to 20 (both sampling site as populations and landscapes as populations), we

223 set a burn-in period of 100,000 followed by additional 1,000,000 iterations, and 20 replicates were

224 run at each *K*. We determined *K* based on the log posterior probability of the data for a given *K*

225   (Pritchard et al. 2000), and on the rate of change in the log probability of the data between

226   successive clusters—the ΔK statistic (Evanno et al. 2005). These analyses were performed in

227   Structure Harvester v.0.6.94 (Earl 2012). All runs were averaged at the best *K* with Clumpp v.1.1.2

228   (Jakobsson and Rosenberg 2007) and results were visualized with Distruct v.1.1 (Rosenberg 2004).

229

230   We inferred historical migration rates using mitochondrial sequences in Migrate-N v.3.6 (Beerli

231   2009). Under a coalescent framework and the infinite allele model, Migrate-N estimates migration

232   rates (measured as a mutation-scaled immigration rate, M) up to ~4 effective population size (Ne)

233   generations (thousands of years). We used slice sampling to run four statistically heated parallel

234   chains (heated at 1.0, 1.5, 3.0, and 1,000,000) for 1,000,000 iterations, and excluded 100,000

235   iterations as burn-in. MCMC estimates of M were modeled with prior boundaries of 0 and 100,000.

236   We used a full migration model and considered parameter estimates accurate when an effective

237   sample size (ESS) >1,000 was observed (Converse et al. 2015). We multiplied the M by the

238   mutation rate, $0.0105*10^{-4}$ for the mitochondrial data (Lovette 2004; Weir and Schluter 2008).

239   To test for spatial auto-correlation of migration rate, we performed a Mantel test with pairwise

240   migration rates and geographic distances (Euclidean) using the *vegan* v. 2.4-3 (Oksanen et al.

241   2010) R package. We performed these analyses both between landscapes and between sampling

242   sites separately.

243

244   To estimate current migration rates, we used the microsatellite data in BayesAss v.3.0 (Wilson and

245   Rannala 2003), which applies a Bayesian approach and MCMC sampling to estimate migration

246   (m) over the last few generations. This analysis was run with 10 million iterations, a sampling

247   frequency of 2,000, a burn-in of 10%, and default settings. We estimated the migration rate

248   between sampling sites and between the three landscapes separately.

249

10

250 Furthermore, to identify if past demographic changes can explain genetic diversity and migration

251 rates, we inferred historical population demography using the Bayesian coalescent skyline plot

252 method (Drummond et al. 2005) as implemented in Beast v.1.8.2 (Drummond et al. 2012). We

253 chose the most suitable substitution model for the mitochondrial data based on Bayesian

254 information criterion (BIC) with jModelTest2 v.2.1.10 (Darriba et al. 2012). We set the

255 substitution model chosen by jModelTest2 (HKY + invariable sites) under a strict-clock model

256 and the general avian substitution rate of mitochondrial evolution of 2.1% sequence divergence

257 per million years (Lovette 2004; Weir and Schluter 2008). Runs of 100 million steps were

258 performed, sampling every 10,000 steps under default settings. Skyline plots were constructed

259 using Tracer v.1.6 (Rambaut and Drummond 2007). We reconstructed historical population size

260 considering all populations together and then separately for Aracá from Viruá + Uatumã following

261 the populations identified with BAPS.

262

263 *Landscape metrics and genetic diversity:* To investigate if landscape metrics predict genetic

264 diversity metrics we calculated genetic metrics through nucleotide diversity (P_i) and haplotype

265 diversity (H_D) from mitochondrial sequences and allelic richness (NG) and genetic diversity

266 (Theta) from microsatellite data. We calculated these metrics within each site and analyzed as a

267 function of the two landscape metrics (habitat amount and proximity index) and of the landscape

268 of origin of each site (Aracá, Viruá our Uatumã).

269

270 Thus for each dependent variable (P_i, H_D, Theta, and NG), we defined a set of models to explain

271 variation in genetic diversity. The final model set included models for each single landscape

272 metric, and additional models with additive and interaction terms of the landscape origin to

273 determine whether landscape context was also an important factor (i.e. to which landscape each

11

274   group of sampling sites belongs to). The final model set also included a constant, intercept-only

275   model, comprising a total of seven models for each dependent variable (Table S3).

276

277   Models were selected using an information theory approach based on AIC (Akaike 1974) and

278   using the corrected AIC (AICc) for small sample sizes (Burnham and Anderson 2002). Models

279   with dAIC = < 2 were considered equally plausible and we used the normalized model weight (wi)

280   to contrast the best model to the constant (no-effect) model. We used generalized linear models

281   (Crawley 2007) with Gaussian error distribution after checking for the distribution of residuals.

282   Before run the analysis landscape metrics were standard to mean = 0 and variance = 1 to make

283   different metrics comparable. The GLM analyses were performed using the *vegan* v. 2.4-3

284   (Oksanen et al. 2010) package and the model selection was made using the *bbmle* v.1.0.20 (Bolker

285   and Bolker 2017) package, both in R.

286

287   *Geographical isolation by distance and by resistance:* To determine if genetic differentiation is

288   better predicted by geographical distance or resistance we calculated the pairwise genetic

289   differentiation F_{ST} (Weir and Cockerham 1984) for both ND2 and microsatellite data between

290   landscapes and among sites within landscapes separately using the *fstat* function in the *Hierfstat*

291   v.0.5.7 R package, with 1,000 permutations to obtain significance (Goudet 2001). To investigate

292   patterns of isolation by geographical distance, we performed Mantel tests in the *vegan* v. 2.4-3 R

293   package. We used a pairwise geographic (Euclidean) and a pairwise genetic distance (F_{ST} values).

294   We performed these analyses both between landscapes and between sampling sites within each

295   landscape separately.

296

297   To investigate the patterns of isolation by resistance we assigned resistance values to vegetation

298   cover within each landscape based on a questionnaire given to four expert Amazonian

299   ornithologists for each landscape category for *E. ruficeps*. Values ranged from 0.01 (less

300   resistance) to 0.99 (more resistance). We took the average resistance value of each landscape

301   category to calculate the isolation by resistance (Table S3). We used the *gdistance* v. 1.2-2 (Etten

302   2017) R package to create the transition layer using the inverse of the sum of each pixel to create

303   the conductance layer (Fig. S1) and the *commuteDistance* function that calculates the expected

304   random-walk commute resistance between nodes in a graph, to create the pairwise resistance

305   matrix for each landscape. We then performed a Mantel test using the pairwise genetic distance

306   (F_{ST} values) against the resistance distance. Additionally, we calculated the minimum resistance

307   distance (i.e, least cost path) for each pair of sites and a Mantel test with the pairwise genetic

308   distances (F_{ST} values).

309

310   **Results**

311

312   *Genetic diversity, structure, and migration:* We obtained 978 bp of the ND2 gene, yielding a total

313   of 178 sequences with 62 variable sites. Haplotype diversity from mitochondrial data of all samples

314   was 0.79 (+/- 0.08) and nucleotide diversity was 0.002 (+/- 0.001). For microsatellite data, we

315   scored the same 178 individuals at 15 loci. No departure of Hardy-Weinberg Equilibrium was

316   detected at any locus and no pair of loci was in linkage disequilibrium (see Table S2 for number

317   of alleles per locus). Aracá landscape had the highest haplotype (0.84 +/- 0.07) and nucleotide

318   diversity (0.003 +/- 0.0006) for mitochondrial data. For microsatellite data Aracá also had the

319   highest allelic richness (24 +/- 3.58) but Viruá had the highest genetic diversity (1.69 +/- 0.04,

320   Table S4).

321

322   We detected low but significant genetic differentiation among landscapes for both mitochondrial

323   and microsatellite data (Table 1). For mitochondrial data, Viruá and Aracá had the largest

13

324   differentiation (F_{ST} = 0.1, p < 0.05), while the largest differentiation for microsatellite data was

325   inferred between Viruá and the Uatumã landscapes (F_{ST} = 0.2, p < 0.05, Table 1). Comparing

326   among all sampling sites, within and among landscapes, mitochondrial results revealed low but

327   significant differentiation among almost all sites within each landscape, except among some Aracá

328   sites (Table S5). Genetic differentiation among sites from different landscapes was highest than

329   sites within landscapes and significant, except between some Uatumã and Viruá sites (Table S5).

330   Microsatellite results revealed several cases of non-significant differentiation among sites, within

331   and among landscapes (Table S6). For sites in different landscapes, the sites from Uatumã were

332   more differentiated than sites of both Aracá and Viruá (Table S6).

333

334   We found 56 mitochondrial haplotypes that grouped into three main clusters. Most haplotypes

335   from Aracá landscape were not shared with the Viruá and Uatumã landscapes, and within Aracá

336   the haplotypes were grouped in two main clusters. Only one Aracá haplotype was shared with the

337   other two landscapes (Fig. 1A). Despite clear differentiation between Aracá and the other two

338   landscapes, the haplotype networks inside each landscape had little or no small-scale geographic

339   structuring. Within each landscape, sampled haplotypes occurred in almost all sampled sites (Fig.

340   1B-D). BAPS results agree with the haplotype networks and inferred K = 3 populations, with two

341   groups within Aracá and one with all haplotypes from Viruá and Uatumã, including three Aracá

342   haplotypes found in five individuals (Fig. 2A), log (marginal likelihood) of optimal partition = -

343   920.3443, 100% probability of K = 3. For microsatellites, the highest log posterior probability of

344   the data and the highest value for ΔK obtained via Structure analysis also inferred K = 3 (Fig. 2B),

345   however the populations recovered by the microsatellite data corresponded to the three sampled

346   landscapes.

347

348   Estimates of historical migration obtained from Migrate-N with mitochondrial data indicated low

349   and asymmetrical gene flow from Uatumã to Viruá (0.0009) and from Viruá to Uatumã (0.0003),

350   with even lower but symmetrical rates between Viruá and Aracá (0.0001 in both directions), and

351   very low rates between Uatumã and Aracá (<0.00006 in both directions; Fig 3A). Estimates of

352   contemporary migration obtained from BayesAss with microsatellite data resulted in high self-

353   recruitment rates for all three landscapes (Aracá = 0.99 [±0.006], Uatumã = 0.67 [±0.005] and

354   Viruá = 0.67 [±0.006]). Contemporary migration was also asymmetrical, with individuals moving

355   mainly from Uatumã and Viruá towards Aracá, 0.32 (±0.008) and 0.32 (±0.009), respectively (Fig.

356   3B). Among all sites, historical ($r = 0$, $p = 0.5$) and contemporary ($r = -0.08$, $p = 0.84$) migration

357   rates were not related with geographic distance (Fig. S2A). Also, among landscapes, contemporary

358   ($r = -0.03$, $p = 0.67$) and historical ($r = 0.16$, $p = 0.67$) migration rates were not significantly related

359   to geographical distance (Fig S2B).

360

361   Finally, analyses based on the mitochondrial data showed demographic expansion for *E. ruficeps*

362   population as a whole. Bayesian skyline plot estimates showed general population expansion over

363   the last 50,000 years (Fig. S3A). When we estimated demography separately, the Aracá population

364   showed the demographic expansion over the last 50,000 years (Fig. S3B), but Viruá and Uatumã

365   populations have maintained their population size constant over time (Fig. S3C).

366

367   *Landscape metrics and genetic diversity:* For the nucleotide diversity metric (Pi), a single best

368   model was selected that contained landscape of origin as the single predictor variable (AICw =

369   0.7686), while for haplotype diversity (H_D) the single best model was the constant intercept-only

370   model (AICw = 0.5573). For microsatellite genetic diversity (Theta), a single best model was

371   selected that contained just landscape of origin as predictor variable (AICw = 0.732) and for allelic

372   richness (NG) the single best model contained de proximity index as the single best predictor

373   variable (AICw = 0.9376, Fig. 4A-D). See respective dAICc and AIC weights in Table 2 and best

374   models estimated parameters in Table S7.

375

376   *Geographical distance, resistance and gene flow:* Genetic distance (F_{ST}) for both microsatellite (r

377   = 0.41, p = 0.01) and mitochondrial (r = 0.48, p = 0.001) data were positively correlated with

378   geographic distance among landscapes (Fig 5A and B). However, no correlation with geographic

379   distance was found among sites within each landscape (Table S8; Fig. 5C and D). No significant

380   relationship was found between genetic differentiation (F_{ST}) and resistance between sites within

381   each landscape, in either dataset (mitochondrial or microsatellite) using the random-walk commute

382   resistance (Table S8; Fig. 5E and F) and the pairwise minimal resistance between the sites.

383

384   **Discussion**

385   We used a set of molecular markers with different evolutionary rates to analyze patterns of genetic

386   diversity and population structure of *Elaenia ruficeps*, a white-sand specialist bird, by sampling

387   three landscapes with different amount and configuration of *campina* patches in central Amazonia,

388   we found that: 1) landscapes harbor genetically distinct populations, with asymmetrical gene flow

389   among them; 2) historical and contemporary estimates of genetic structure and migration rates

390   differ, implying dynamic connections among landscapes through time; 3) overall genetic structure

391   (diversity and differentiation) is best explained by a regional effect (i.e. landscape of origin), than

392   by habitat configuration, except for allelic richness which increases with patch proximity (more

393   connectivity), supporting some evidence for local movement restriction between isolated patches;

394   and 4) genetic differentiation increases with geographical distance among landscapes, whereas

395   within landscapes no isolation by distance or by resistance is detected although small genetic

396   differentiations is detected among patches. That suggests that dispersal of *E. ruficeps* between

397   *campina* patches is restricted at least to some degree locally, but gene flow may be much more

398   hampered by dispersal limitation at regional scales (between landscapes). Thus, our results stress

399   the high complexity in *E. ruficeps* population dynamics in a habitat with insular nature.

400

401   *Genetic diversity and population structure: historical influences*

402   The landscape with greatest habitat amount, Aracá, had the highest mitochondrial nucleotide (Pi)

403   and haplotype (H_D) diversity, and two mtDNA populations recovered in population structure

404   analyses (Fig. 1A; Fig. 2A). A similar pattern of high genetic diversity and population structure

405   was found for another white-sand specialist bird, *Xenopipo atronitens,* in the same region

406   (Capurucho et al. 2013). Thus, it is likely that historical landscape alterations, such as glacial

407   cycles, may have caused past population isolation within the Aracá landscape.

408

409   Population expansion starting around 50,000 years before present (Fig. S2) was found for *E.*

410   *ruficeps* in our analyses, in agreement with other Amazonian bird species from *campinas*

411   (Capurucho et al. 2013; Matos et al. 2016), but in contrast to results obtained for the same species

412   using two additional nuclear markers (Ritter et al. 2020). This difference may be due to the lower

413   mutation rates of nuclear markers (Allio et al. 2017), and increased sampling per locality used

414   here. These historical demographic changes indicate that the populations of *E. ruficeps* may have

415   started expanding in the last inter glacial, before the Last Glacial Maximum (LGM; Clark et al.

416   2009). When demography was estimated separately for each landscape, Aracá showed

417   demographic expansion over the last 50,000 years (Fig. S3B), whereas Viruá + Uatumã showed

418   constant population size (Fig. S3C), suggesting that glacial cycles incurred variable impact in

419   different regions of Amazonia and may explain the highest P_i, due to population expansion, in

420   Aracá.

421

17

422   Studies on both northern (Carneiro Filho et al. 2002; Horbe, Horbe and Suguio 2004; Teeuw and

423   Rhodes 2004; Zular et al. 2019) and southern (Latrubesse 2002) Amazonian *campinas* indicate

424   that this habitat responded to historical changes in climate, with the strongest signal detected in

425   the north. An increase in sediment deposition, primarily from the Tepuis, and aeolian activity, on

426   northern *campinas* (Teeuw and Rhodes 2004; Zular et al. 2019), could have increased connectivity

427   among populations of white-sand specialist species by increasing the area and connectivity of

428   campinas, and consequently increasing population size and genetic diversity, during drier climatic

429   periods in the Aracá region. Contrastingly, the Viruá landscape currently has the highest Theta

430   diversity. *Campina* patches in Viruá also have higher diversity of white-sand specialist bird

431   species, possibly due to its proximity to other open habitat types such as the Northern South

432   America savannas (Fig. 1; Borges et al. 2016a; Capurucho et al. 2020a).

433

434   Estimated migration rates were asymmetrical, as found for other Amazonian birds (Capurucho et

435   al. 2013; Menger et al. 2017), and we also found distinct values for historical and contemporary

436   migration. Historical migration was higher between Uatumã and Viruá, with rates from Uatumã to

437   Viruá three-fold higher than from Viruá to Uatumã. The Aracá landscape appears to be historically

438   isolated from the other two landscapes. The historical isolation of Aracá may be explained by

439   alterations to its overall size and/or connectivity during the Pleistocene glacial cycles (Teeuw and

440   Rhodes 2004) and by the Branco River formation (Cremon et al. 2016). The Branco River is a

441   white-water river that separates Aracá from Uatumã and Viruá and, together with its floodplains

442   covered by seasonally flooded várzea vegetation, appear to have a stronger resistance for

443   *campina's* specialist birds (Capurucho et al. 2013; Matos et al. 2016). Furthermore, as suggested

444   by haplotype network and migration rates, both previously (Ritter et al. 2020) and in this study,

445   this river is also a barrier for *E. ruficeps*, which may have limited historical migration for Aracá

446   populations. Analyses of sedimentary deposits and regional geomorphology suggested that a long

447 segment of the Branco River was established in Late Pleistocene (Cremon et al. 2016). The initial

448 establishment of the Branco River at about 30 kya may have collaborated to increased isolation of

449 the Aracá population, but with gradual development of floodplain vegetation the barrier effect may

450 be less pronounced since then. It is also possible that with the *terra-firme* canopy cover becoming

451 less dense during past drier periods (Cowling et al. 2001), as hypothesized for northern Amazonia

452 during the LGM (Häggi et al. 2017), the forested matrix surrounding *campinas* may have also

453 turned more permeable than flooded forests along the Branco River, allowing for larger migration

454 between Viruá and Uatumã, while Aracá remained isolated.

455

456 In summary, Pleistocene glacial cycles are a likely driver of population dynamics in of *E. ruficeps*

457 through the increase of individual mobility across *terra-firme* forests in dry periods, while in the

458 more isolated Aracá landscape, the continuous availability of the white-sand areas, even in wetter

459 periods, may explain the higher genetic diversity. Genetic diversity patterns found for *E. ruficeps*

460 are congruent with findings from other white-sand specialist birds (Capurucho et al. 2013; Matos

461 et al. 2016), corroborating the idea that Pleistocene glacial cycles have deeply influenced

462 Amazonian biogeographical history, and shaped current inter and intra-specific diversity (Rangel

463 et al. 2018). This combined evidence from white-sand specialist birds suggests a dynamic

464 interaction between closed canopy forests, open forests and non-forest / open vegetation areas

465 (Cowling et al 2011; Arruda et al 2017), indicating that past climatic change deeply influenced

466 Amazonian biogeographic history, and contradicting previous suggestions of a stable landscape in

467 Amazonia during the Quaternary (Smith et al 2014).

468

469 *Genetic diversity and population structure: contemporary influences*

470

19

471   In contrast to the historical scenario, microsatellite data indicate that current migration occurs

472   primarily from Uatumã and Viruá towards Aracá, with lower migration rates in all other directions.

473   Asymmetrical gene-flow arises due to more favorable dispersal conditions in one direction or due

474   to source-sink dynamics across heterogeneous environments (e.g., Oswald et al. 2017; Hauser et

475   al. 2019; Moussy et al. 2018). Aracá has the largest area of *campina* vegetation and is the most

476   internally connected landscape. Furthermore, Aracá has in general the largest genetic diversity as

477   measured here by three of the four indices, and in this context Aracá could function as a source

478   population with a higher rate of emigration from Aracá towards the other populations. However,

479   we found the opposite pattern, a higher migration rate towards Aracá, the largest and more

480   connected population.

481

482   Considering the recent population expansion documented in Aracá over the last 50,000 years, in

483   contrast to stability of population sizes in Uatumã and Viruá, it is possible that dispersal of

484   individuals towards Aracá may be the result of emigration from small *campina* patches with little

485   resource availability (e.g., Uatumã) or from landscapes that have been more affected by human

486   impact (e.g., Viruá) with overall lower carrying capacity, but that are still able to maintain stable

487   populations and thus are probably not sinks. Therefore, the asymmetrical gene flow in our study

488   is most likely not consistent with a source-sink dynamic, and other mechanism should be

489   investigated. An increased cost for dispersing towards one direction, as observed along elevational

490   gradients (Cheviron and Brumfield 2009) is unlikely in our study system, but it is possible that

491   environmental fluctuations are less strong in northern Amazonia (Jimenez and Takahashi 2019),

492   leading to more constant resource supply in Aracá (the northern most landscape).

493

494   Landscape structure and landscape features have been shown to be important in shaping genetic

495   diversity at the local scale for Amazonian vertebrates (e.g., Bates 2002; Capurucho et al. 2013;

496   Menger et al. 2018; Silva et al. 2020). Here we show that allelic richness (NG) decreased in more

497   isolated *campina* patches, but with no effect of habitat amount, in contrast to other findings

498   showing that habitat amount best predicts genetic diversity and species diversity in white-sand

499   specialist bird communities (Capurucho et al. 2013, Borges et al. 2016a).

500

501   This suggests that current local movements of *E. ruficeps* are, at least to certain degree, shaped by

502   the configuration of *campina* patches. However, for *Xenopipo atronitens* another white-sand

503   specialist bird, haplotype and nucleotide diversity increased with the amount of habitat available,

504   with no effect of configuration (Capurucho et al. 2013). This difference may be explained by

505   different species traits and habitat use patterns, since *X. atronitens* individuals also use

506   *campinarana*, those white-sand patches that have taller vegetation than *campinas*, and eventually

507   exploit black-water flooded forests as well (Oren 1981; Ridgely and Tudor 2009). In contrast, *E.*

508   *ruficeps* is more restricted to *campina* vegetation (Borges et al. 2016b). Additionally, *E. ruficeps*

509   has a lower handwing index than *X. atronitens*, a trait that was found to be correlated with overall

510   range size in white-sand specialist birds (Capurucho et al. 2020b). These differences in habitat

511   use highlight the importance of considering species traits when addressing congruence in

512   biogeographical scenarios (Papadopoulou and Knowles 2016). Thus, we conclude that white-sand

513   specialist birds are affected by landscape structure, but different components of these landscapes

514   influence movement patterns of different species and both habitat amount (for *X. atronitens*;

515   Capurucho et al 2013) and configuration (for *E. ruficeps*; this study) appear to be important for

516   driving spatial patterns of genetic diversity of these white-sand specialist birds.

517

518   Genetic distance among landscapes increased with larger geographic distances in both

519   mitochondrial and microsatellite data. Although significant genetic differentiation was found

520   among most sampling sites within landscapes, no pattern of isolation by distance or resistance was

21

521   observed. More refined studies on habitat permeability for white-sand vegetation birds are needed

522   to develop more accurate isolation by resistance models. Our results suggest that although

523   dispersal ability of *E. ruficeps* is at least to certain degree restricted through intervening vegetation

524   types (Ritter et al. 2020), it is still greater than overall dispersal ability for most *terra-firme* forest

525   birds (Menger et al. 2017; Menger et al. 2018), but dispersal ability of *E. ruficeps* is lower when

526   compared to dispersal of savanna birds (Bates et al. 2003; Ritter et al. 2020). In a previous study

527   comparing the population structure of *E. ruficeps* with its sister species *E. cristata*, it was evident

528   that *E. cristata* populations that occur in savanna, have a low population structure indicating a

529   higher mobility than *E. ruficeps* (Ritter et al. 2020). Furthermore, birds that occur in the *terra-*

530   *firme* forest are generally limited by geographic distance (e.g. Menger et al. 2017; Menger et al.

531   2018), while typical Amazonian open area (savannas) bird species appear to have low population

532   genetic structure, even at large geographic distances and across biogeographical barriers (Bates et

533   al. 2003; Ritter et al. 2020).

534

535   **Conclusions**

536

537   Here, we infer population structure, genetic diversity and migration within *E. ruficeps,* a white-

538   sand specialist bird, among three Amazonian landscapes, using both, mitochondrial and

539   microsatellite data. Distinct population structure was found for the different markers used,

540   indicating differences in historical and current patterns of connectivity among landscapes.

541   Migration rates were asymmetrical and also indicated a distinct scenario in the past compared to

542   current rates. Patch isolation within and among landscapes was important to explain spatial

543   patterns of microsatellite genetic diversity (NG). Geographical distance limited dispersal among

544   but not within landscapes. These results suggest that both current landscape structure and the

545   history of *campina* patches determine genetic diversity patterns of *campina* specialist birds.

546 Further studies will certainly foster our understanding of how biotic communities associated to

547 white-sand patches are influenced by current and historical processes in Amazonia, considering

548 that these communities will probably be affected by future climatic changes.

549

550 **Acknowledgments**

551 We thank the Brazilian authorities, ICMBio (20524-3 ICMBio/MMA), CEUC-AM, PARNA

552 Viruá, and RDS Uatumã (24597-2 ICMBio/MMA) for providing the collecting permits and

553 logistical support, and Fundação Vitória Amazônica (FVA), and Instituto de Conservação e

554 Desenvolvimento Sustentável do Amazonas (Idesam) for logistical support. Laboratory work was

555 conducted at the Laboratório Temático de Biologia Molecular (LTBM-INPA). Genetic data were

556 gathered in the Pritzker Laboratory for Molecular Systematics and Evolution at the Field Museum

557 of Natural History (FMNH). We thank Arielle Machado to read an initial version of the manuscript

558 and Josué Azevedo for help with isolation by resistance analysis. We thank Gisiane Lima, João

559 Capurucho, and Thiago Laranjeiras to answer the questionnaire about matrix resistance values.

560

561 **Declarations:**

562 **Funding:** FAPESP and FAPEAM for financial support through the 'Fapesp-Fapeam' joint

563 funding program (FAPESP 09/53365-0). CDR thanks the financial support from Alexander von

564 Humboldt Foundation and CNPq (Conselho Nacional de Desenvolvimento Científico e

565 Tecnológico - Brazil: 249064/2013-8). CCR is supported by a productivity fellowship from CNPq.

566 C.D.B. is supported by the Swedish Research Council (2017-04980). During the execution of this

567 study SHB received a grant from FAPEAM (Fixam program, Edital no. 017/2014).

568 **Conflicts of interest/Competing interests:** The authors declare no conflicts or competing of

569 interests.

23

570   **Ethical approvals:** ICMBio, CEUC-AM (20524-3 ICMBio/MMA),, PARNA Viruá, and RDS

571   Uatumã (24597-2 ICMBio/MMA) for collecting permits.

572   **Consent to participate:** All authors declare to consent to participate of this study.

573   **Consent for publication:** All authors declare to consent the publication of this study.

574   **Availability of data material:** GenBank accession ND2 sequences ID: 2304423. Microsatellite

575   data is available in Ritter *et al.* 2014.

576   **Code availability:** Not applicable.

577   **Authors contribution:** C.C., C.C.R., C.D.R., and S.H.B. designed the study. C.D.R. and J.M.

578   generated and analyzed the data. C.D.R. wrote the manuscript with contribution of C.C., C.C.R.,

579   C.B., J.M., J.P.M., J.B., and S.H.B.

580

References

Adeney JM, Christensen NL, Vicentini A, Cohn-Haft M (2016) White-sand ecosystems in Amazonia. Biotropica 48:7–23

Allio R, Donega S, Galtier N, Nabholz B (2017) Large variation in the ratio of mitochondrial to nuclear mutation rate across animals: implications for genetic diversity and the use of mitochondrial DNA as a molecular marker. Mol Biol Evol 34:2762–2772

Anderson AB (1981) White-sand vegetation of Brazilian Amazonia. Biotropica 13:199–210

Antonelli A, Zizka A, Carvalho FA, et al (2018) Amazonia is the primary source of Neotropical biodiversity. Proc Natl Acad Sci 115:6034–6039. https://doi.org/10.1073/pnas.1713819115

Avise JC (2009) Phylogeography: retrospect and prospect. J Biogeogr 36:3–15

Bates JM (2002) The genetic effects of forest fragmentation on five species of Amazonian birds. J Avian Biol 33:276–294

Bates JM, Tello JG, Silva JMC (2003) Initial assessment of genetic diversity in ten bird species of South American Cerrado. Stud Neotrop Fauna Environ 38:87–94

Beerli P (2009) How to use MIGRATE or why are Markov chain Monte Carlo programs difficult to use. Popul Genet Anim Conserv 17:42–79

Bicudo TC, Sacek V, de Almeida RP, et al (2019) Andean tectonics and Mantle Dynamics as a Pervasive Influence on Amazonian ecosystem. Sci Rep 9:1–11

Biomatters (2012) Geneious version 5.6. 5 created by Biomatters

Bolker B, Bolker M Ben (2017) Package 'bbmle.' Tools Gen Maximum Likelihood Estim 641:

Borges SH, Cornelius C, Moreira M, et al (2016a) Bird communities in Amazonian white-sand vegetation patches: effects of landscape configuration and biogeographic context. Biotropica 48:121–131

Borges SH, Cornelius C, Ribas C, et al (2016b) What is the avifauna of Amazonian white-sand vegetation? Bird Conserv Int 26:192–204

606   Capurucho JMG, Borges SH, Cornelius C, et al (2020a) Patterns and processes of diversification

607   in Amazonian white sand ecosystems: insights from birds and plants. In: Neotropical

608   Diversification: Patterns and Processes. Springer, pp 245–270

609   Capurucho JMG, Ashley M V, Tsuru BR, et al (2020b) Dispersal ability correlates with range

610   size in Amazonian habitat-restricted birds. Proc R Soc B 287:20201450

611   Capurucho JMG, Cornelius C, Borges SH, et al (2013) Combining phylogeography and

612   landscape genetics of Xenopipo atronitens (Aves: Pipridae), a white sand campina

613   specialist, to understand Pleistocene landscape evolution in Amazonia. Biol J Linn Soc

614   110:60–76

615   Carneiro Filho A, Schwartz D, Tatumi SH, Rosique T (2002) Amazonian paleodunes provide

616   evidence for drier climate phases during the Late Pleistocene–Holocene. Quat Res 58:205–

617   209

618   Cheng H, Sinha A, Cruz FW, et al (2013) Climate change patterns in Amazonia and biodiversity.

619   Nat Commun 4:1411

620   Cheviron ZA, Brumfield RT (2009) Migration-selection balance and local adaptation of

621   mitochondrial haplotypes in rufous-collared sparrows (Zonotrichia capensis) along an

622   elevational gradient. Evol Int J Org Evol 63:1593–1605

623   Clark PU, Dyke AS, Shakun JD, et al (2009) The last glacial maximum. Science (80-) 325:710–

624   714

625   Clement MJ, Snell Q, Walker P, et al (2002) TCS: estimating gene genealogies. In: ipdps. p 184

626   Converse PE, Kuchta SR, Roosenburg WM, et al (2015) Spatiotemporal analysis of gene flow in

627   Chesapeake Bay Diamondback Terrapins (Malaclemys terrapin). Mol Ecol 24:5864–5876

628   Corander J, Marttinen P, Sirén J, Tang J (2013) BAPS: Bayesian analysis of population structure.

629   Finl Univ Helsinki

630   Costa FM, Terra-Araujo MH, Zartman CE, et al (2020) Islands in a green ocean: Spatially

631   structured endemism in Amazonian white-sand vegetation. Biotropica 52:34–45

632 Cowling SA, Maslin MA, Sykes MT (2001) Paleovegetation simulations of lowland Amazonia

633   and implications for neotropical allopatry and speciation. Quat Res 55:140–149

634 Cremon ÉH, de Fátima Rossetti D, de Oliveira Sawakuchi A, Cohen MCL (2016) The role of

635   tectonics and climate in the late Quaternary evolution of a northern Amazonian River.

636   Geomorphology 271:22–39

637 Darriba D, Taboada GL, Doallo R, Posada D (2012) jModelTest 2: more models, new heuristics

638   and parallel computing. Nat Methods 9:772

639 DiLeo MF, Wagner HH (2016) A landscape ecologist's agenda for landscape genetics. Curr

640   Landsc Ecol Reports 1:115–126

641 Drummond AJ, Rambaut A, Shapiro B, Pybus OG (2005) Bayesian coalescent inference of past

642   population dynamics from molecular sequences. Mol Biol Evol 22:1185–1192

643 Drummond AJ, Suchard MA, Xie D, Rambaut A (2012) Bayesian phylogenetics with BEAUti

644   and the BEAST 1.7. Mol Biol Evol 29:1969–1973

645 Earl DA (2012) STRUCTURE HARVESTER: a website and program for visualizing

646   STRUCTURE output and implementing the Evanno method. Conserv Genet Resour 4:359–

647   361

648 Etten J van (2017) R package gdistance: distances and routes on geographical grids

649 Evanno G, Regnaut S, Goudet J (2005) Detecting the number of clusters of individuals using the

650   software STRUCTURE: a simulation study. Mol Ecol 14:2611–2620

651 Excoffier L, Laval G, Schneider S (2005) Arlequin (version 3.0): an integrated software package

652   for population genetics data analysis. Evol Bioinforma 1:117693430500100000

653 Fahrig L (1998) When does fragmentation of breeding habitat affect population survival? Ecol

654   Modell 105:273–292

655 Fine PVA, García-Villacorta R, Pitman NCA, et al (2010) A floristic study of the white-sand

656   forests of Peru. Ann Missouri Bot Gard 283–305

657   Frankham R, Briscoe DA, Ballou JD (2002) Introduction to conservation genetics. Cambridge

658   university press

659   Goudet J (2001) FSTAT, a program to estimate and test gene diversities and fixation indices,

660   version 2.9. 3. http//www2 unil ch/popgen/softwares/fstat htm

661   Goudet J, Jombart T (2015) hierfstat: estimation and tests of hierarchical F-statistics. R Packag

662   version 004-22

663   Gruber B, Henle K (2008) Analysing the effect of movement on local survival: a new method

664   with an application to a spatially structured population of the arboreal gecko Gehyra

665   variegata. Oecologia 154:679–690

666   Gustafson EJ, Parker GR (1994) Using an index of habitat patch proximity for landscape design.

667   Landsc Urban Plan 29:117–130

668   Häggi C, Chiessi CM, Merkel U, et al (2017) Response of the Amazon rainforest to late

669   Pleistocene climate variability. Earth Planet Sci Lett 479:50–59

670   Hansen MC, Potapov P V, Moore R, et al (2013) High-resolution global maps of 21st-century

671   forest cover change. Science (80-) 342:850–853

672   Hauser SS, Walker L, Leberg PL (2019) Asymmetrical gene flow of the recently delisted

673   passerine black-capped vireo (Vireo atricapilla) indicates source-sink dynamics in central

674   Texas. Ecol Evol 9:463–470

675   Horbe AMC, Horbe MA, Suguio K (2004) Tropical Spodosols in northeastern Amazonas State,

676   Brazil. Geoderma 119:55–68

677   Hubisz MJ, Falush D, Stephens M, Pritchard JK (2009) Inferring weak population structure with

678   the assistance of sample group information. Mol Ecol Resour 9:1322–1332

679   Hulce D, Li X, Snyder-Leiby T, Liu CSJ (2011) GeneMarker® genotyping software: Tools to

680   increase the statistical power of DNA fragment analysis. J Biomol Tech JBT 22:S35

681   Itescu Y (2019) Are island-like systems biologically similar to islands? A review of the

682   evidence. Ecography (Cop) 42:1298–1314

683   Jakobsson M, Rosenberg NA (2007) CLUMPP: a cluster matching and permutation program for

684   dealing with label switching and multimodality in analysis of population structure.

685   Bioinformatics 23:1801–1806

686   Jimenez JC, Takahashi K (2019) Tropical Climate Variability and Change: Impacts in the

687   Amazon. Front Earth Sci 7:215

688   Latrubesse EM (2002) Evidence of Quaternary palaeohydrological changes in middle Amazônia:

689   the Aripuanã-Roosevelt and Jiparaná" fans". ZEITSCHRIFT FUR Geomorphol Suppl 61–

690   72

691   Leigh JW, Bryant D (2015) popart: full-feature software for haplotype network construction.

692   Methods Ecol Evol 6:1110–1116

693   Librado P, Rozas J (2009) DnaSP v5: a software for comprehensive analysis of DNA

694   polymorphism data. Bioinformatics 25:1451–1452

695   Lovette IJ (2004) Mitochondrial dating and mixed support for the "2% rule" in birds. Auk

696   121:1–6

697   Manicacci D, Olivieri I, Perrot V, et al (1992) Landscape ecology: population genetics at the

698   metapopulation level. Landsc Ecol 6:147–159

699   Matos M V, Borges SH, d'Horta FM, et al (2016) Comparative phylogeography of two bird

700   species, Tachyphonus phoenicius (Thraupidae) and Polytmus theresiae (Trochilidae),

701   specialized in Amazonian white-sand vegetation. Biotropica 48:110–120

702   McGarigal K, Cushman SA, Neel MC, Ene E (2002) FRAGSTATS: spatial pattern analysis

703   program for categorical maps. Comput Softw Progr Prod by authors Univ Massachusetts,

704   Amherst Available Follow web site www umass edu/landeco/research/fragstats/fragstats

705   html 6:

706   McRae BH (2006) Isolation by resistance. Evolution (N Y) 60:1551–1561

707   Menger J, Henle K, Magnusson WE, et al (2017) Genetic diversity and spatial structure of the Rufous-throated Antbird (Gymnopithys rufigula), an Amazonian obligate army-ant follower. Ecol Evol 7:2671–2684

710   Menger J, Unrein J, Woitow M, et al (2018) Weak evidence for fine-scale genetic spatial structure in three sedentary Amazonian understorey birds. J Ornithol 159:355–366

712   Moussy C, Arlettaz R, Copete JL, et al (2018) The genetic structure of the European breeding populations of a declining farmland bird, the ortolan bunting (Emberiza hortulana), reveals conservation priorities. Conserv Genet 19:909–922

715   Myster RW (2016) The physical structure of forests in the Amazon Basin: a review. Bot Rev 82:407–427

717   Oksanen J, Blanchet FG, Kindt R, et al (2010) Vegan: community ecology package. R package version 1.17-4. http//cran r-project org> Acesso em 23:2010

719   Oren DC (1981) Zoogeographic analysis of the white sand campina avifauna of Amazonia

720   Oswald JA, Overcast I, Mauck III WM, et al (2017) Isolation with asymmetric gene flow during the nonsynchronous divergence of dry forest birds. Mol Ecol 26:1386–1400

722   Papadopoulou A, Knowles LL (2016) Toward a paradigm shift in comparative phylogeography driven by trait-based hypotheses. Proc Natl Acad Sci 113:8018–8024

724   Prance GT (1996) Islands in Amazonia. Philos Trans R Soc London Ser B Biol Sci 351:823–833

725   Press E (2005) Linear Referencing in ArcGIS: ArcGIS 9. Esri Press

726   Pritchard JK, Stephens M, Donnelly P (2000) Inference of population structure using multilocus genotype data. Genetics 155:945–959

728   R Core Team (2015) R: A language and environment for statistical computing.

729   Rambaut A, Drummond AJ (2007) Tracer v1. 4: MCMC trace analyses tool

730   Rangel TF, Edwards NR, Holden PB, et al (2018) Modeling the ecology and evolution of

biodiversity: biogeographical cradles, museums, and graves. Science (80-) 361:eaar5452

Raymond M, Rousset F (1995) Population genetics software for exact test and ecumenicism. J Hered 86:248–249

Rheindt FE, Norman JA, Christidis L (2008) Phylogenetic relationships of tyrant-flycatchers (Aves: Tyrannidae), with an emphasis on the elaeniine assemblage. Mol Phylogenet Evol 46:88–101

Ridgely RS, Tudor G (2009) Field guide to the songbirds of South America: the passerines. University of Texas Press

Ritter CD, Coelho LA, Capurucho JM, et al (2020) Sister species, different histories: comparative phylogeography of two bird species associated with Amazonian open vegetation. Biol J Linn Soc. https://doi.org/10.1093/biolinnean/blaa167

Ritter CD, Figueiredo CMÉ, Gubili C, et al (2014) Isolation and characterization of seventeen polymorphic microsatellite DNA markers from Elaenia ruficeps (Aves: Tyrannidae). Conserv Genet Resour 6:. https://doi.org/10.1007/s12686-014-0273-x

Ritter CD, Zizka A, Roger F, et al (2018) High-throughput metabarcoding reveals the effect of physicochemical soil properties on soil and litter biodiversity and community turnover across Amazonia. PeerJ 2018:e5661. https://doi.org/10.7717/peerj.5661

Rocha DG da, Kaefer IL (2019) What has become of the refugia hypothesis to explain biological diversity in Amazonia? Ecol Evol 9:4302–4309

Ronce O (2007) How does it feel to be like a rolling stone? Ten questions about dispersal evolution. Annu Rev Ecol Evol Syst 38:231–253

Rosenberg NA (2004) DISTRUCT: a program for the graphical display of population structure. Mol Ecol Notes 4:137–138

Rousset F (2008) genepop'007: a complete re-implementation of the genepop software for Windows and Linux. Mol Ecol Resour 8:103–106

756 Silva SM, Ferreira G, Pamplona H, et al (2020) Effects of landscape heterogeneity on population

757   genetic structure and demography of Amazonian phyllostomid bats. Mammal Res 1–9

758 Silva SM, Peterson AT, Carneiro L, et al (2019) A dynamic continental moisture gradient drove

759   Amazonian bird diversification. Sci Adv 5:eaat5752

760 Sorenson MD, Ast JC, Dimcheff DE, et al (1999) Primers for a PCR-based approach to

761   mitochondrial genome sequencing in birds and other vertebrates. Mol Phylogenet Evol

762   12:105–114

763 Tautz D (1989) Hypervariability of simple sequences as a general source for polymorphic DNA

764   markers. Nucleic Acids Res 17:6463–6471

765 Teeuw RM, Rhodes EJ (2004) Aeolian activity in northern Amazonia: optical dating of Late

766   Pleistocene and Holocene palaeodunes. J Quat Sci Publ Quat Res Assoc 19:49–54

767 Tuomisto H, Van Doninck J, Ruokolainen K, et al (2019) Discovering floristic and geoecological

768   gradients across Amazonia. J Biogeogr 46:1734–1748

769 Van Houtan KS, Pimm SL, Halley JM, et al (2007) Dispersal of Amazonian birds in continuous

770   and fragmented forest. Ecol Lett 10:219–229

771 Wang X, Edwards RL, Auler AS, et al (2017) Hydroclimate changes across the Amazon

772   lowlands over the past 45,000 years. Nature 541:204

773 Weir BS, Cockerham CC (1984) Estimating F-statistics for the analysis of population structure.

774   Evolution (N Y) 38:1358–1370

775 Weir JT, Schluter D (2008) Calibrating the avian molecular clock. Mol Ecol 17:2321–2328

776 Wilson GA, Rannala B (2003) Bayesian inference of recent migration rates using multilocus

777   genotypes. Genetics 163:1177–1191

778 Wright S (1943) Isolation by distance. Genetics 28:114

779 Zular A, Sawakuchi AO, Chiessi CM, et al (2019) The role of abrupt climate change in the

780   formation of an open vegetation enclave in northern Amazonia during the late Quaternary.

781   Glob Planet Change 172:140–149

782

783

784   Tables:

785   Table 1 – F_{ST} among landscapes. Values above the diagonal are microsatellite F_{ST} and below the

786   diagonal are ND2 sequence F_{ST}. All values are significant at $P < 0.05$.

	Arcacá	Uatumã	Viruá
Aracá	-	0.0194	0.0102
Uatumã	0.09732	-	0.0201
Viruá	0.10579	0.00507	-

787

788 Table 2 – Variables used in model selection with their respective delta dAICc and weight values. The best fit model has a
789 dAICc = 0 is present in bold as the alternative good models (dAICc =< 2). The genetic diversity variables for mitochondrial
790 data are nucleotide diversity (Pi) and haplotype diversity and for the microsatellite data are Theta and NG. The independent
791 variables are Habitat amount and Proximity index. The model used landscape as a fixed factor or as interacting variable.

| Model	Variables	Pi		H$_D$		Theta		NG	
		dAICc	Weight	dAICc	Weight	dAICc	Weight	dAICc	Weight
M0	Constant	21	<0.001	**0**	**0.5573**	5.4	0.049	6.9	0.0294
M1	Landscape	**0**	**0.7686**	3.6	0.093	**0**	**0.732**	10.9	0.0039
M2	Habitat amount	23.7	<0.001	2.1	0.1981	7.7	0.016	9.8	0.0069
M3	Proximity	23.3	<0.001	3	0.1226	6.7	0.025	**0**	**0.9376**
M4	Landscape + habitat amount	4.1	0.0986	7.1	0.0157	4.1	0.093	15.2	<0.001
M5	Landscape * habitat amount	13.2	0.001	12.5	0.0011	15.6	<0.001	24	<0.001
M6	Landscape + Proximity	3.5	0.1307	7.7	0.012	4.3	0.084	7.6	0.0213
M7	Landscape * Proximity	13.2	0.0011	16	<0.001	13.7	<0.001	15.9	<0.001

792
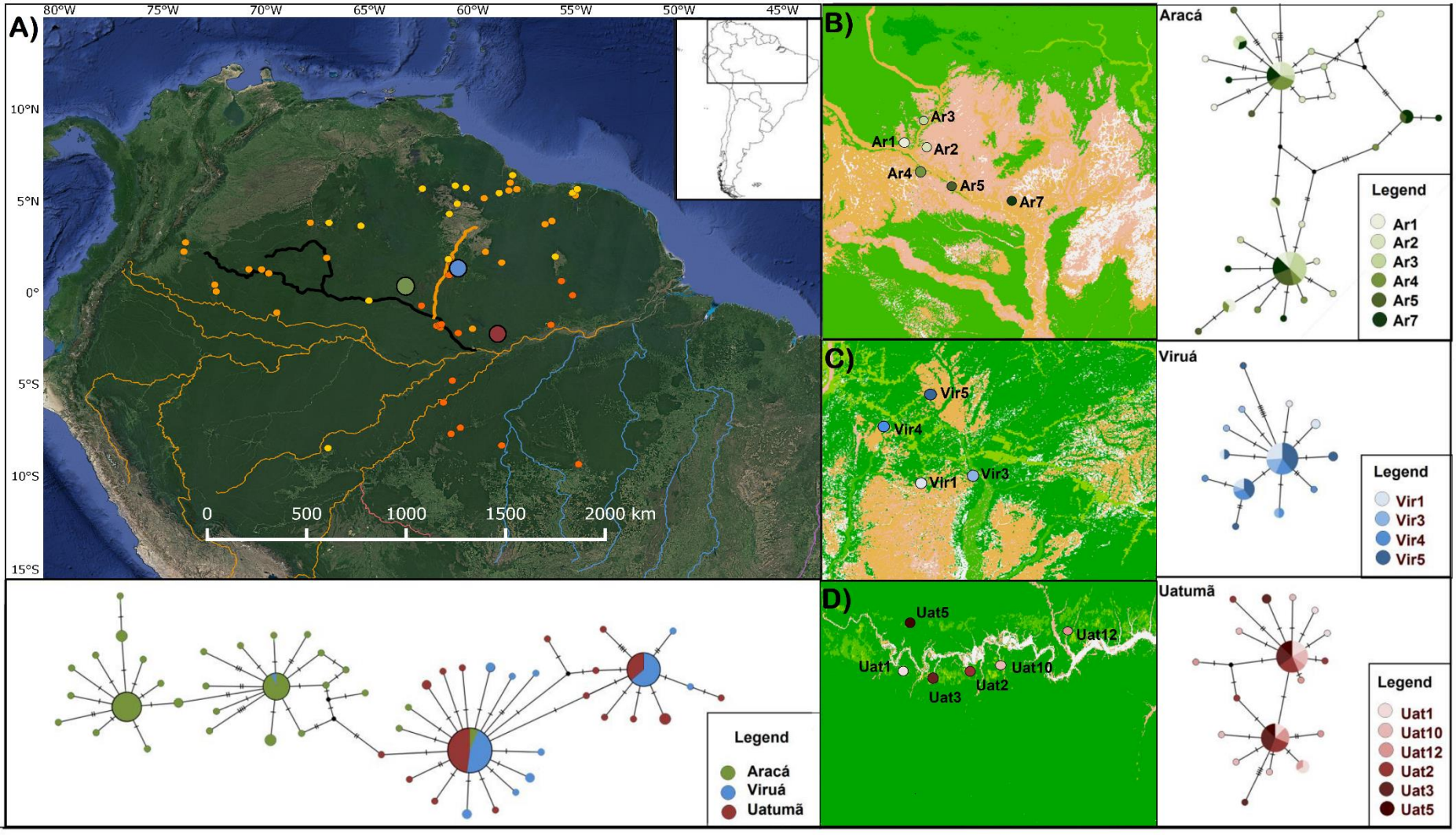
Figure 1A) – Map of the distribution of *Elaenia ruficeps*. Points in yellow are from the Global Biodiversity Information Facility (GBIF) public database (general and potentially biased by mis-identification); points in bright orange are from museum collections (highly curated locality information). Points in dark orange are areas with available tissue samples. Points in green, blue, and red are the landscapes sampled in this study (Aracá, Viruá, and Uatumã respectively). The main rivers of the Amazon basin are shown according with their water color; rivers with high sediment concentration are brown, with low sediment concentration are blue. We highlight the Negro river in Black and the Branco river in brown both with tick lines. B) shows in detail the sites sampled in Aracá with the respective haplotype network; C) shows the sites sampled in Viruá with the respective haplotype network and; and D) shows the sites sampled on Uatumã and the respective haplotype network.
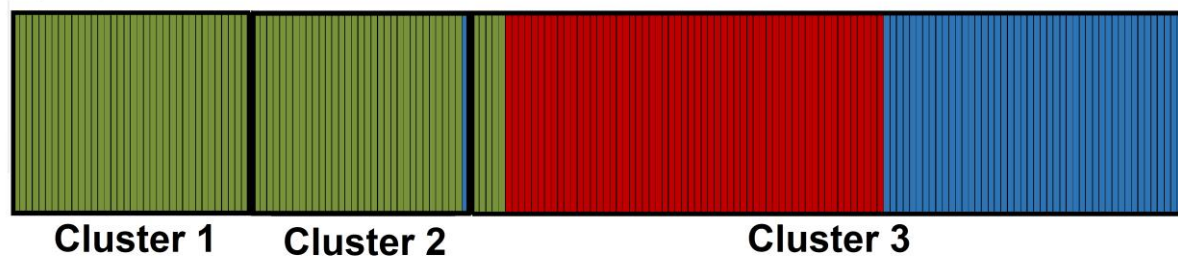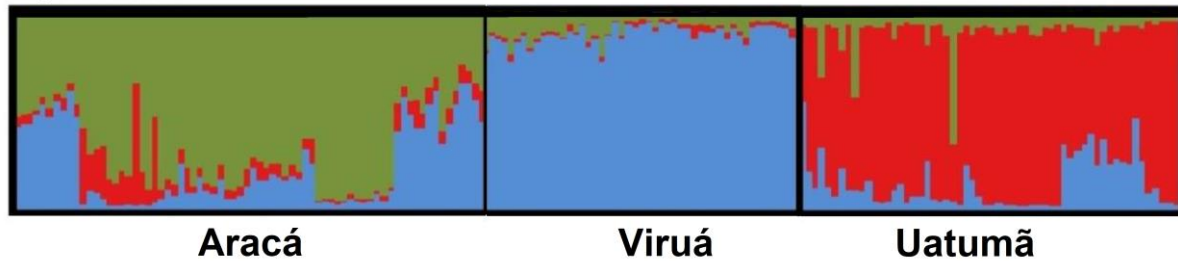
Figure 2 - Population structure of *Elaenia ruficeps* based on (A) mtDNA (BAPS) with individuals ordered by cluster membership and colored by landscape of origin (landscapes in decreasing order of *campina* habitat coverage: Aracá = green, Viruá = blue, Uatumã = red), and (B) microsatelites (Structure), for which clusters match the different landscapes. In both analyses recorded $K = 3$ genetic clusters, which are delimited by thick black lines.
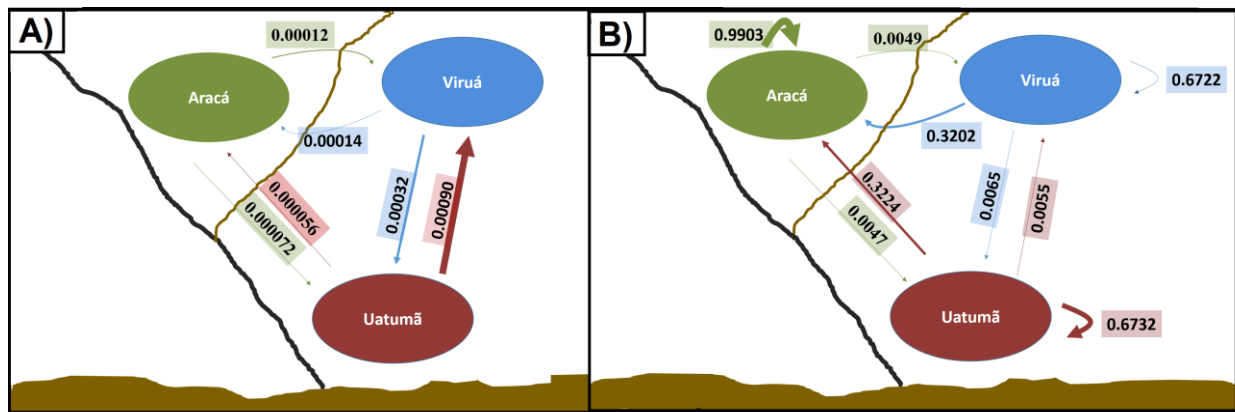
Figure 3 – Pairwise migration rates. A) Historical migration rate calculated for mtDNA ND2 sequences in Migrate-N. B) Contemporary migration rate calculated in BayesAss using microsatellite data (CM microsatellite). The size of the arrows is proportional to the migration estimates. Black line represents Negro River and brow line the Branco River. Brown coloration in the bottom of figure represents the Amazon River. Historical migration shows the highest migration rate between Uatumã and Viruá, while contemporary migration shows higher migration from Uatumã and Viruá to Aracá.
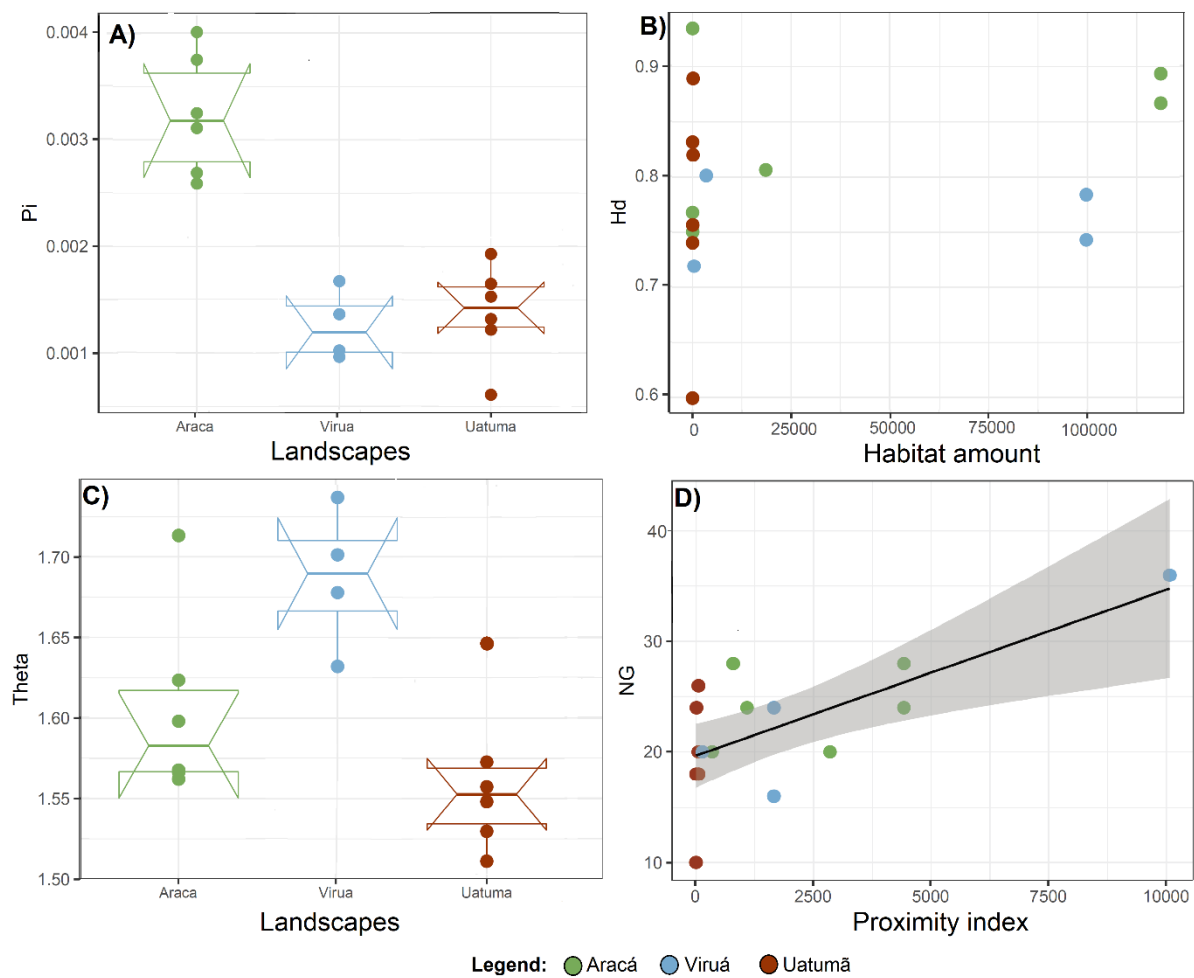
Figure 4 – Best models about the source of variation of mitochondrial (A and B) and microsatellite (C and D) genetic diversity among sites within landscapes (Aracá = green, Viruá = blue, Uatumã = red). A) nucleotide diversity (P_i) based on ND2 is best explained by landscape; B) haplotype diversity based on ND2 sequences and habitat amount in m^2 (but none of the predictor variables explained haplotype diversity; the constant model was selected as the best model). C) Theta from microsatellite data is best explained by landscape, and D) the microsatellite genetic diversity (NG) is best explained by the Proximity index.
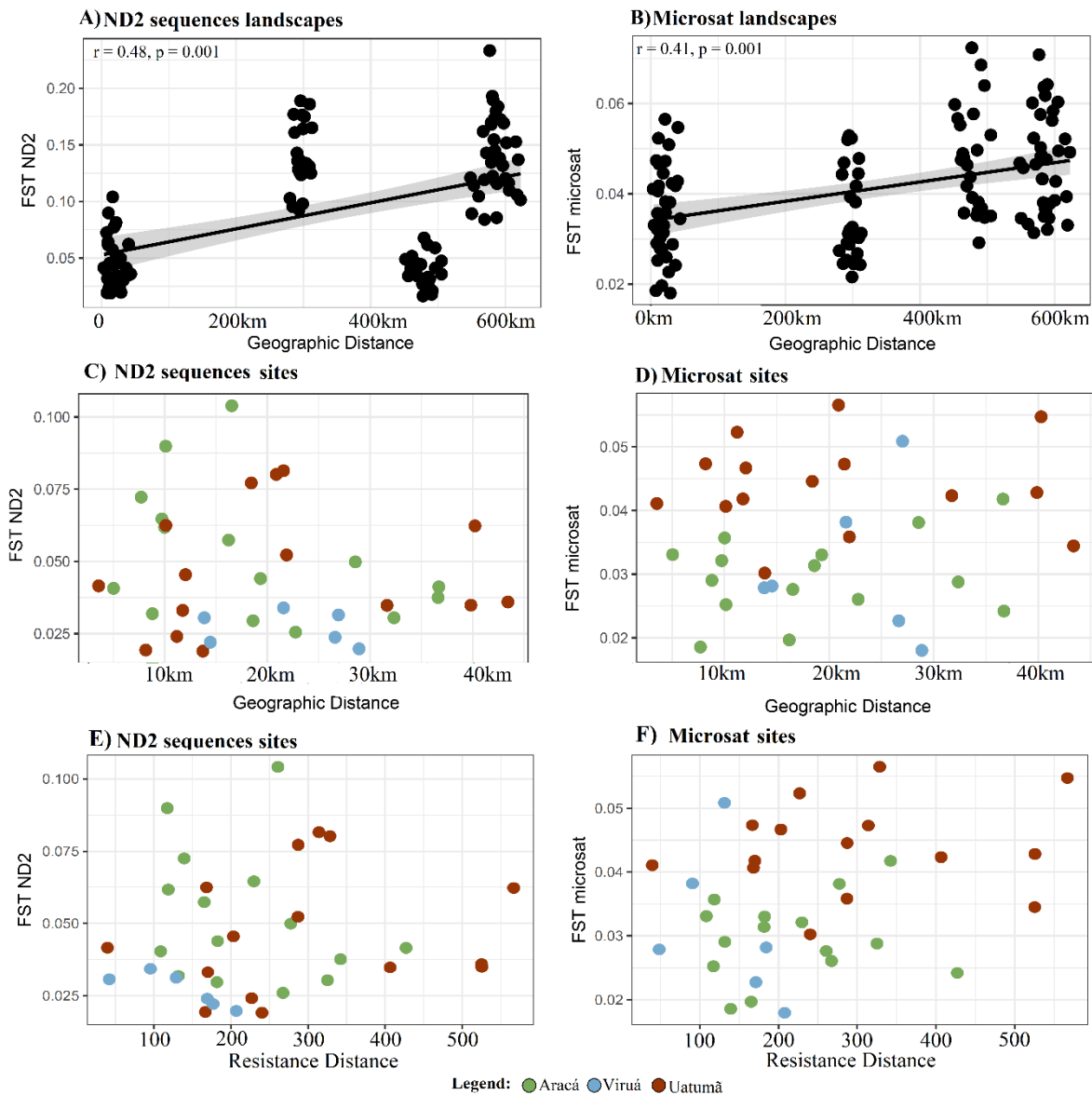
Figure 5 – Pairwise genetic distance (FST) and geographical distance relationship calculated with Mantel test. A) F_{ST} from ND2 sequence data and B) microsatellite data both plotted against the geographical distance between landscapes. C) F_{ST} from ND2 sequence data and D) microsatellite data both plotted against the geographical distance between sites inside each landscape. E) F_{ST} from ND2 sequence data and F) microsatellite data both plotted against the resistance distance between sites inside each landscape. The geographical distance is just significant between landscapes. Above pairwise matrix for all sites and below the data from each landscape: green = Aracá; blue = Viruá and; red = Uatumã.